Fingerprint Segmentation using the Phase of Multiscale Gabor Wavelets

Sylvain Bernard[1,2], Nozha Boujemaa[1], David Vitale[2], Claude Bricot[2]

[1] INRIA Rocquencourt BP 105, F-78153 Le Chesnay, France
[2] THALES Identification, 41 bd de la Republique, BP 53- 78401 Chatou Cedex, France
sylvain.bernard@inria.fr

Abstract

Most automatic systems for fingerprint identification are based on minutiae matching. Minutiae points are terminaisons and bifurcations of the ridge lines that constitute a fingerprint pattern. A critical step in fingerprint matching is to automatically and reliably extract minutiae from the input fingerprint image. The efficiency of minutiae detection depends on how well the ridges and valleys are extracted. The result of this segmentation process is a binarized image. In our present work, we propose a multiscale Gabor wavelet filter bank for a robust and efficient fingerprint segmentation. After a brief presentation of the Gabor wavelet theory, we explain how ridges and valleys are distinguished in terms of the phase, this being the key point of our binarization process. Moreover, the multiscale approach provides noise elimination whilst preserving singularities that characterize minutiae. Finally, we have evaluated the performance of our minutiae extraction algorithm using the accuracy of an online fingerprint verification system.

1. Introduction

Several approaches for automatic minutiae detection have been proposed. In [1], Maio and Maltoni propose a direct gray-scale minutiae detection based on a ridge line following algorithm. However, the vast majority of proposed methods consists in first detecting ridges and valleys, providing a binarized image that is skeletonized for automatic minutiae extraction. The binarization process requires image enhancement, then a threshold based decision distinguishes ridges and valleys.

In [2], O'Gorman and Nickerson present an enhancement technique based on the convolution of the image with a filter oriented according to the directional image. In [3], Sherlock, Monro and Millard propose a directional filtering process in the Fourier domain. The more precise approach proposed in [4] takes the local frequency into account using a local Fourier transform. The method is efficient but time consuming. To speed up the process, the authors have to use overlapping windows creating local discontinuities in the binarized image. In [5], Hong, Wan and Jain present a technique based on local projections on an even-symmetric Gabor filter tuned to the local direction and local frequency. Those features are calculated in advance in each pixel neighborhood.

In our present work, we propose a Gabor wavelet filter bank for local direction and frequency extraction. Unlike in [5], the obtained phase is required for fingerprint binarization. Moreover, our multiscale approach provides noise elimination whilst preserving singularities that characterize minutiae.

2. Brief Presentation of Gabor Wavelets

2.1- Unidimensional Gabor Wavelets

Consider a square summable function *g(t)* of time t, $t \in \left]-\infty,+\infty\right[$, composed of **local** frequencies. A localized frequency is one having a finite support. In such a signal, the Fourier transform is not suitable for frequency detection and localization. Indeed, the Fourier transform consists in global projections on sinusoidal waves having no localization parameters. We prefer projections on Gabor wavelets *h*, having a frequency parameter ω_0 , a localization t_0 and a scale parameter σ that influences wavelet support size (Fig.1) [6]:

$$h(\omega_0, t_0, \sigma)(t) = \frac{1}{\sqrt{\sigma}} \cdot e^{-\frac{(t-t_0)^2}{2\cdot\sigma^2}} \cdot e^{i\cdot\omega_0\cdot t}.$$

Consider H, the Fourier transform of *h* :

$$H(\omega_0, t_0, \sigma)(\omega) = \sqrt{2\cdot\pi} \cdot e^{-\frac{\sigma^2\cdot(\omega-\omega_0)^2}{2}} \cdot e^{i\cdot t_0\cdot(\omega-\omega_0)}$$

We remark that a Gabor wavelet is a **bandpass** filter centered on the ω_0 frequency (Fig.1).

Gabor wavelet functions $\{h(\omega_0, t_0, \sigma)\}_{\omega_0, t_0, \sigma}$ do not form a basis of square summable functions.

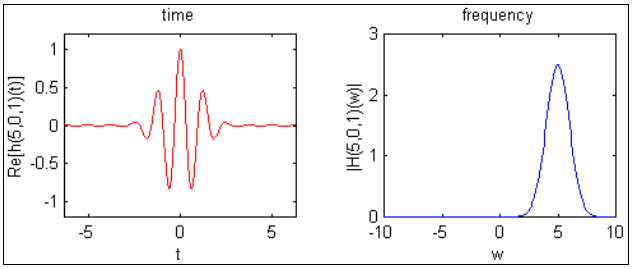

Fig.1 – A Gabor Wavelet and its Fourier transform

2.2- Bidimensional Gabor Wavelets

Consider a bidimensional Gabor wavelet $g_{\omega,\theta}(x,y)$ of frequency ω and orientation θ.

$$g_{\omega,\theta}(x,y) = \frac{1}{\sqrt{\sigma_{\theta_\perp}}} \cdot e^{-\frac{v^2}{2\cdot\sigma_{\theta_\perp}{}^2}} \cdot \frac{1}{\sqrt{\sigma_\theta}} \cdot e^{-\frac{u^2}{2\cdot\sigma_\theta{}^2}} \cdot e^{i\cdot\omega\cdot u}$$

with $u = x\cdot\cos(\theta) + y\cdot\sin(\theta)$

$v = -x\cdot\sin(\theta) + y\cdot\cos(\theta)$

$\sigma_\theta, \sigma_{\theta^\perp}$ are scale parameters in the direction of the wave and in its orthogonal direction respectively.

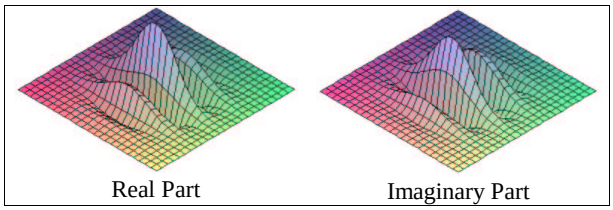

Fig.2 – A bidimensional Gabor wavelet

We remark that : $g_{\omega,\theta}(u,v) = L(v)\cdot B(u)$ where *B(u)* is the equation of a bandpass filter, centered on the ω frequency, and *L(v)* is the equation of a gaussian low-pass filter. A bidimensional Gabor wavelet is composed of a **bandpass** filter in the direction of the wave and a **lowpass** filter in the orthogonal direction (Fig.2).

3. Application to Fingerprint Identification

3.1- Domain Specific Knowledge

Fingerprint images are composed of ridges and valley creating an oriented and periodic texture.
To demonstrate that two fingerprints are from the same finger or not, human experts detect the ridge ending and bifurcation points of both fingerprints (Figs.3,4). These points are called minutiae [7].

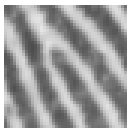

Fig.3 – Ridge Ending

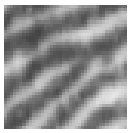

Fig.4 – Ridge Bifurcation

For fingerprint comparison, the two minutiae sets are matched by superposition to count the number of common points. Two fingerprints are considered to be from the same finger if the number of common points is sufficient, depending on the country's legislation.

3.2- Wavelets for Minutiae Detection

In our present work, we do not directly detect the minutiae as done in [1]. The reason why we prefer to extract ridges and valleys first is that we take advantage of the strong **a-priori** information on the local shape of fingerprints. Fingerprints are locally composed of an oriented and periodic structure that we model with a Gabor wavelet. The θ and ω parameters of the wavelet are given by a local features extraction process.

3.2.1- Local features extraction

In [5], the authors propose a first detection of the local direction θ, using Sobel masks, then a detection of the frequency ω, by computing the x-signature. The method is computationally efficient but an error on the estimation of the direction generates an incorrect frequency.

We propose local projections on a **bank** of Gabor wavelet filters having 8 different orientations and 3 different frequencies. The bank respects the independence of the direction and frequency variables. The filter that gives the best coefficient of projection is selected and provides the local direction θ and local frequency ω (Figs.5,6).

At each point (x_0, y_0), consider a pixel neighborhood *f* of size *W.W.* $f(x,y)$ represents the image intensity at pixel $(x_0 + x, y_0 + y), (x,y) \in [-W/2, W/2]^2$.

- We first normalize f to a constant energy and obtain the function f':

$$f'(x,y) = \frac{V}{v(x_0,y_0)} \cdot [f(x,y) - m(x_0,y_0)],$$ *m* is the mean value and *v* is the variance of *f*.

Thus, the mean value of f' is equal to 0 and its norm is independent of (x_0, y_0) (Eqn.1).

$$\|f'\| = \sqrt{\frac{1}{W^2}\int_{-\frac{W}{2}}^{\frac{W}{2}}\int_{-\frac{W}{2}}^{\frac{W}{2}} f'(x,y)^2 \cdot dx \cdot dy} = V \quad \text{(Eqn.1)}$$

- Then, we compute the local projections of f' on each of the 24 filters of the bank (Fig.5). The projection of f' on a Gabor wave of frequency ϖ and direction α is a complex number :

$$A_{\varpi,\alpha} e^{i\cdot\varphi_{\varpi,\alpha}} = \frac{\int_{-\frac{W}{2}}^{\frac{W}{2}}\int_{-\frac{W}{2}}^{\frac{W}{2}} f'(x,y)\cdot g_{\varpi,\alpha}(x,y)\cdot dx\cdot dy}{\|f'\|\cdot\|g_{\varpi,\alpha}\|} \quad \text{(Eqn.2)}$$

with $A_{\varpi,\alpha} \in [0,1]$ and $\varphi_{\varpi,\alpha} \in [0,2\pi[$

We empirically chose *W=11* to have a correct noise reduction. To speed up the process, we calculate in advance $\|g_{\varpi,\alpha}\|$ and $\|f'\|$ because of their independence of (x_0, y_0).

Thus, for a given point (x_0, y_0), we obtain the following features : $(\omega,\theta) = \underset{\varpi,\alpha}{\text{Argmax}}\, A_{\varpi,\alpha}$

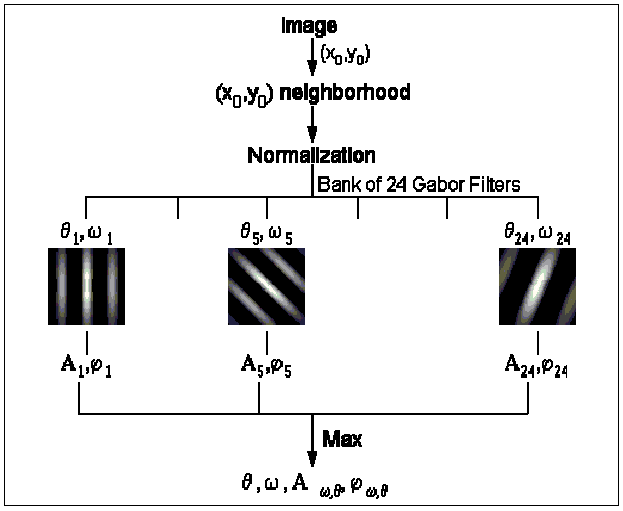

Fig.5 – Scheme of Gabor filters bank

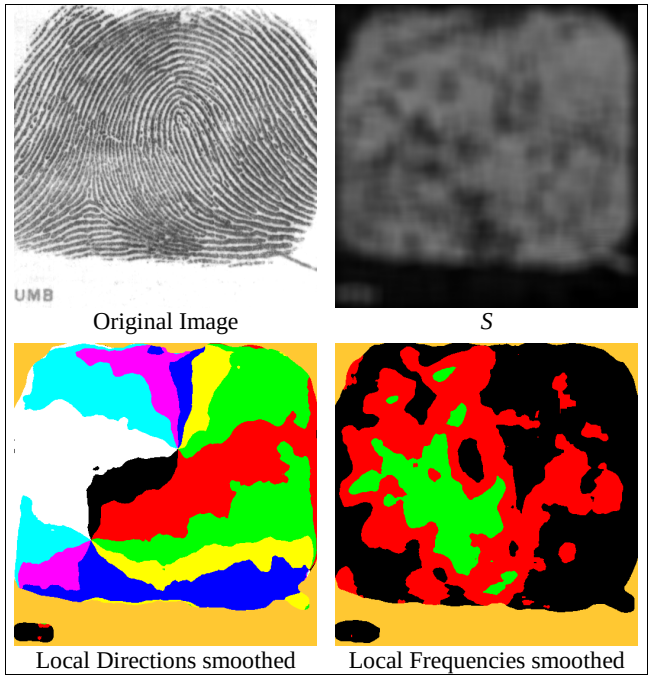

Fig.6 – Outputs of the Filter bank

3.2.2- Fingerprint Segmentation

The segmentation process is divided in two steps :

❶ A first detection of background/noisy area and the Region of Interest (ROI) of the print (Fig.7).

At each pixel, we calculate the local direction θ, the frequency ω, and the associated coefficient of projection $A_{\omega,\theta}$. We obtain three images and apply a low-pass filter for noise reduction (Fig.6). Consider *S*, the smoothed image of coefficients.

Because the energy of each pixel neighborhood is normalized (Eqn.1), the coefficients $A_{\omega,\theta}$ (Eqn.2) are not influenced by the local contrast of the print. Thus, we use two global thresholds T_1 and T_2 $(0 < T_1 < T_2 < 1)$ to carry out a first segmentation of the image. For each pixel (x_0, y_0),

- if $S(x_0, y_0) \in [0, T_1[$, it means that the pixel neighborhood does not have an oriented and periodic structure, the point is a background point.
- if $S(x_0, y_0) \in [T_1, T_2[$, the pixel neighborhood has a weak oriented and periodic structure, the point lies in a noisy area.

- if $S(x_0, y_0) \in]T_2, 1]$, the neighborhood of the given point has a strong oriented and periodic structure. The point is therefore situated in the ROI of the print.

This segmentation avoids the detection of false minutiae in noisy areas. Moreover, the number of noisy pixels relative to the number of ROI pixels gives a global quality score that is used for automatic rejection of low quality prints.

❷ At each point of the ROI, the binarization step consists of deciding if the given point should belong to a ridge or a valley on the real finger of the person. At each pixel (x_0, y_0) of the ROI, the filter having the best coefficient of projection provides the local direction θ, the local frequency ω, the magnitude $A_{\omega,\theta}$ and the **phase** information $\varphi_{\omega,\theta}$. We obtain a sinusoidal model of the local signal in the pixel neighborhood :

$$A_{\omega,\theta} \cos\left(\omega \cdot [\cos(\theta) \cdot (x - x_0) + \sin(\theta) \cdot (y - y_0)] - \varphi_{\omega,\theta}\right)$$

From this model, we can decide if the given point should belong to a ridge or a valley. Because the mean value of each pixel neighborhood is normalized to 0 (Eqn.1), we apply a threshold based decision at 0 : if the sign of the model at point (x_0, y_0) is positive, the point belongs to a ridge; if the sign is negative, the point belongs to a valley. We remark that this decision is highly depending on the **phase** information.

Unfortunately, such a binarization process can artificially connect ridges around minutiae points (Fig.8) that can be the cause of confusion between a ridge ending and a bifurcation point. This information is essential for the matching process. A combinaison of **multiscale** filters is required :

- in a region containing no minutiae, the size of the filter has to be large to eliminate noise
- in a region containing minutiae, a small filter size preserves the singularity characterizing a minutiae.

We have no prior knowledge about minutiae location but we know that they constitute a local discontinuity in the periodic and oriented structure. As a consequence, $A_{\omega,\theta}$ has to be small around minutiae points (Fig.8). But, in case of noisy pixels, we are in the same situation.

We infer the following rule : consider two thresolds T_3 and T_4 and a pixel (x_0, y_0) situated in a subregion of the ROI containing a small amount of noise, such that $1 > S(x_0, y_0) > T_3 > T_2$; if $A_{\omega,\theta}(x_0, y_0)$ is lower than a threshold T_4, we apply a Gabor wavelet tuned to ω and θ, with reduced σ_θ and $\sigma_{\theta^\perp}$ parameters and in a window of size $W=5$. We obtain a new phase, and a new model of the pixel neighborhood. We use the same decision process to distinguish a ridge and a valley.

3.3- Experimental results

On Fig.7 is presented an example of segmented print. A zoom on critical parts of the image shows the improvements of the multiscale approach (Fig.8). From the segmented image, a skeletonization of the black lines provides an efficient detection of the print minutiae.

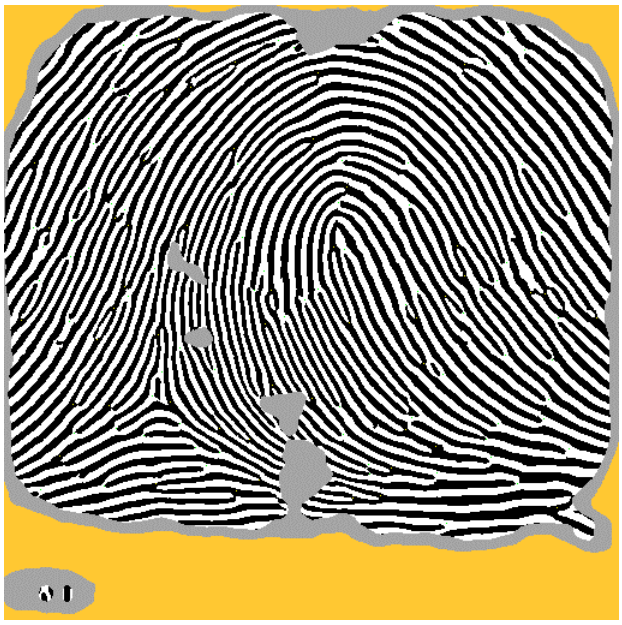

Fig. 7 - Segmented print into background (clear gray), noisy areas (dark gray), ridges (black) and valleys (white)

The performance of the segmentation process was **numerically** assessed using the accuracy of our verification system. Indeed, we have developed a matching algorithm [8] based on a generalized Hough transform [9] and a similarity metric that takes the geometric relationships between minutiae into account. For a given database, the distribution of the matching scores for the same fingers and for different fingers is computed. Setting different values of the threshold on the matching score, we obtain the curves of False Acceptance Rate (Far) and False Rejection Rate (Frr) given by Fig.9.

For comparison to other existing systems, we tested our system on Db1 and Db2 databases of the FVC2000 Competition [10]. We reached the **second position** in the competition by achieving Equal Error Rates (EER) [10] of 3.16% and 1.85% on Db1 and Db2 respectively.

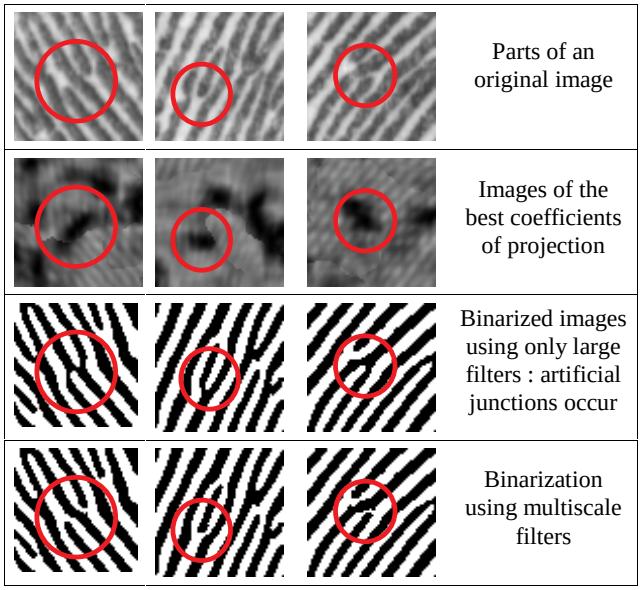

Fig. 8 – Improvements of a multiscale approach

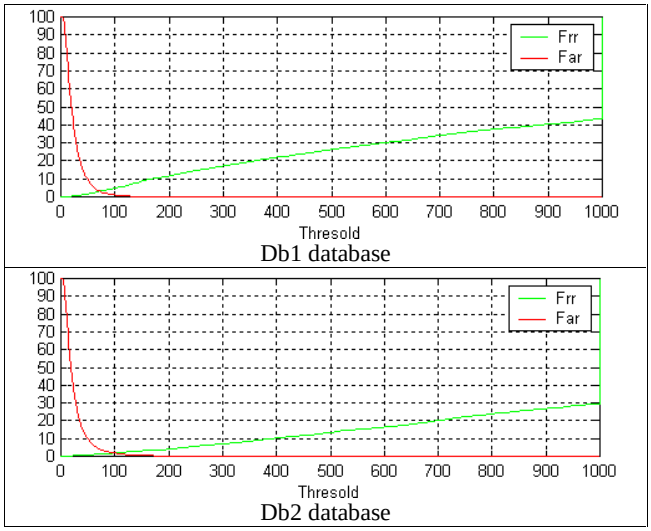

Fig.9 – Far and Frr function of the decision threshold

Conclusion

A Gabor wavelet filter bank is efficient for fingerprint feature extraction. Indeed, it provides :

- a robust fingerprint segmentation into background/ noisy area and the ROI. It avoids the detection of false minutiae in noisy areas and gives a global quality score that is used for the automatic rejection of low quality prints.
- a model of the local signal in each pixel neighborhood of the ROI. From this model, we decide if the given point should belong to a ridge or valley and this decision is highly depending on the phase information.

Moreover, our multiscale approach provides an efficient noise elimination whilst preserving singularities that characterize minutiae. The result is a segmented image that gives minutiae points after a skeletonization step of the extracted ridges.
Since the evaluation of our algorithms in comparison with other verification systems is very encouraging, the results of our researches are integrated into the THALES Identification products. Indeed, this company plans to produce an authentication terminal by incorporating our algorithms onto specific embedded hardware for fingerprint identification.

References

[1]- D. Miao and D. Maltoni, "Direct Gray-Scale Minutiae Detection in Fingerprints", IEEE Trans. PAMI, vol. 19, no. 1, 1997.

[2]- L. O'Gorman and J.V Nickerson , "An Approach to Fingerprint Filter Design", Pattern Recognition, vol. 22, no. 1, pp. 29-38, 1989.

[3]- B.G Sherlock, D.M Monro and K. Millard, "Fingerprint Enhancement by Directional Fourier Filtering", Proc. Conf. Vision, Image and Signal Processing, pp. 87-94, 1994.

[4]- C.I Watson, G.T Candela and P.J Grother, "Comparison of FFT Fingerprint Filtering Methods for Neural Network Classification", NIST technical report no. 5493, 1994.

[5]- L. Hong, Y. Wan and A.K. Jain, "Fingerprint Image Enhancement : Algorithm and Performance Evaluation", IEEE Trans. PAMI, vol. 20, no. 8, pp.777-789, 1998.

[6]- Y. Meyer, "Les Ondelettes - Algorithmes et Applications", Armand Colin, 1994.

[7]- The Science of Fingerprints
US Department of Justice – FBI

[8]- S. Bernard, C. Nastar, N. Boujemaa, D. Vitale and C. Bricot, "Fingerprint Image Retrieval in Very Large Databases", IEEE Workshop on Automatic Identification Advanced Technologies, pp. 95-98, Summit, 1999.

[9]- N.K Ratha, K. Karu, S. Chen and A.K Jain, "A Real-time Matching System for Large Fingerprint Databases", IEEE Trans. PAMI, vol. 18, no. 8, pp.799-813, 1996.

[10]- D. Maio, D. Maltoni, R. Cappelli, J.L Wayman and A.K. Jain, "FVC2000 : Fingerprint Verification Competition", ICPR, Barcelona, September 2000, http://www.bias.csr.unibo.it/fvc2000.